INTEGRATION OF SOLAR PV AND BATTERY STORAGE USING A MULTI-LEVEL INVERTER WITH SVPWM CONTROL

B. Rajashekar[1], P. Balakishan[2]

[1] *Student, EEE Department, Jyothismathi Institute of technology & Science, Telangana, India*
[2] *Assoc.Prof, EEE Department, Jyothismathi Institute of technology & Science, Telangana, India*

ABSTRACT

In this paper a simplified Configuration of a three-level neutral-point-clamped (NPC) inverter that be capable of integrate solar photovoltaic (PV) amid battery storage in a grid-connected system is anticipated. The strong point of the anticipated topology lies in a novel, extended unbalance three-level vector modulation modus operandi amid the purpose of can generate the accurate ac voltage under unbalanced dc voltage conditions. This dissertation presents the propose philosophy of the anticipated Configuration and the notional construction of the anticipated modulation modus operandi A new control algorithm for the anticipated system is also obtainable in order to control the power delivery between the solar PV, battery, and grid, which concurrently provides maximum power point tracking (MPPT) function for the solar PV.

Keyword: - *Solar PV, Battery, NPC Inverter, MPPT*

1. INTRODUCTION

Due to the world energy crisis and environmental problems caused by conventional power generation, renewable energy sources such as photovoltaic (PV) and wind generation systems are becoming more promising alternatives to replace conventional generation units for electricity generation.

Advanced power electronic systems are needed to utilize and develop renewable energy sources. In solar PV or wind energy applications, utilizing maximum power from the source is one of the most important functions of the power electronic systems. In three-phase applications, two types of power electronic configurations are commonly used to transfer power from the renewable energy resource to the grid: single-stage and double-stage conversion.

In the double-stage conversion for a PV system, the first stage is usually a dc/dc converter. The authors are with the Endeavour Energy Power Quality and Reliability second stage is a dc/ac inverter. The function of the dc/dc converter is to facilitate the maximum power point tracking (MPPT) of the PV array and to produce the appropriate dc voltage for the dc/ac inverter. The function of the inverter is to generate three-phase sinusoidal voltages or currents to transfer the power to the grid in a grid-connected solar PV system or to the load in a stand-alone system.

In the single-stage connection, only one converter is needed to full-fill the double-stage functions, and hence the system will have a lower cost and higher efficiency, however, a more complex control method will be required. The current norm of the industry for high power applications is a three-phase, single stage PV energy systems by using a voltage-source converter (VSC) for power conversion.

One of the major concerns of solar and wind energy systems is their unpredictable and fluctuating nature. Grid-connected renewable energy systems accompanied by battery energy storage can overcome this concern. This also can increase the flexibility of power system control and raise the overall availability of the system. Usually, a converter is required to control the charging and discharging of the battery storage system and another converter is required for dc/ac power conversion;

Thus, a three-phase PV system connected to battery storage will require two converters. This paper is concerned with the design and study of a grid-connected three-phase solar PV system integrated with battery storage using only one three-level converter having the capability of MPPT and ac-side current control, and also the ability of controlling the battery charging and discharging. This will result in lower cost, better efficiency and increased flexibility of power flow control.

Numerous industrial applications have begun to require higher power apparatus in recent years. Some medium voltage motor drives and utility applications require medium voltage and megawatt power level. For a medium voltage grid, it is troublesome to connect only one power semiconductor switch directly. As a result, a multilevel power converter structure has been introduced as an alternative in high power and medium voltage situations. A multilevel converter not only achieves high power ratings, but also enables the use of renewable energy sources. Renewable energy sources such as photovoltaic, wind, and fuel cells can be easily interfaced to a multilevel converter system for a high power application. The term multilevel began with the three-level converter. Subsequently, several multilevel converter topologies have been developed. However, the elementary concept of a multilevel converter to achieve higher power is to use a series of power semiconductor switches with several lower voltage dc sources to perform the power conversion by synthesizing a staircase voltage waveform. Capacitors, batteries, and renewable energy voltage sources can be used as the multiple dc voltage sources. The commutation of the power switches aggregate these multiple dc sources in order to achieve high voltage at the output; however, the rated voltage of the power semiconductor switches depends only upon the rating of the dc voltage sources to which they are connected.

A multilevel converter has several advantages over a conventional two-level converter that uses high switching frequency pulse width modulation (PWM). The attractive features of a multilevel converter can be briefly summarized as follows.

● Staircase waveform quality: Multilevel converters not only can generate the output voltages with very low distortion, but also can reduce the dv/dt stresses; therefore electromagnetic compatibility (EMC) problems can be reduced.

● Common-mode (CM) voltage: Multilevel converters produce smaller CM voltage; therefore, the stress in the bearings of a motor connected to a multilevel motor drive can be reduced. Furthermore, CM voltage can be eliminated by using advanced modulation strategies.

● Input current: Multilevel converters can draw input current with low distortion.

● Switching frequency: Multilevel converters can operate at both fundamental switching frequency and high switching frequency PWM. It should be noted that lower switching frequency usually means lower switching loss and higher efficiency.

Unfortunately, multilevel converters do have some disadvantages. One particular disadvantage is the greater number of power semiconductor switches needed. Although lower voltage rated switches can be utilized in a multilevel converter, each switch requires a related gate drive circuit. This may cause the overall system to be more expensive and complex.

Multilevel converter is classified into three types. They are:

1) Cascaded H-bridges converter with separate dc sources

2) Diode clamped (neutral-clamped)

3) Flying capacitors (capacitor clamped).

Abundant modulation techniques and control paradigms have been developed for multilevel converters such as

- sinusoidal pulse width modulation (SPWM),
- selective harmonic elimination (SHE-PWM),
- Space-Vector Modulation (SVM) and others.

• In addition, many multilevel converter applications focus on industrial medium-voltage motor drives, utility interface for renewable energy systems, flexible AC transmission system (FACTS), and traction drive systems.

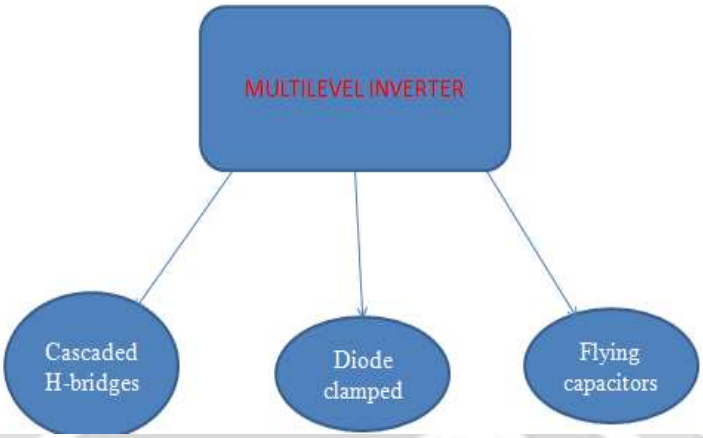

Fig-1: Types of multilevel conveters.

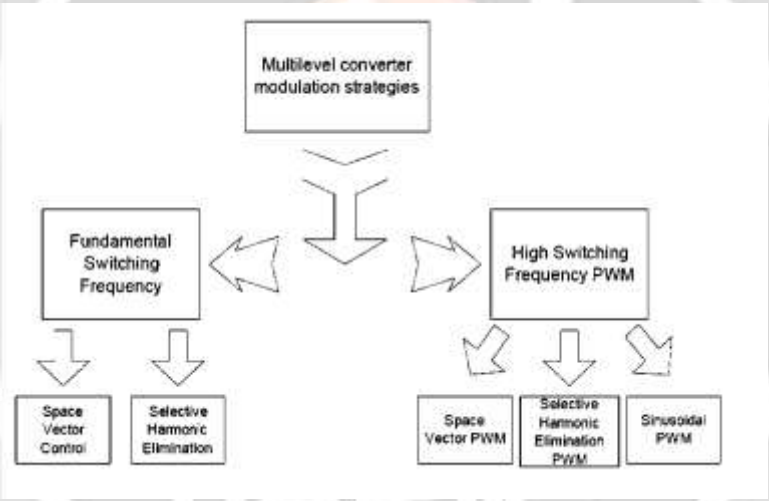

Fig-2: modulation strategies of multilevel converters.

2. PROPOSED TECHNIQUE

The Space Vector PWM generation module accepts modulation index commands and generates the appropriate gate drive waveforms for each PWM cycle. This section describes the operation and configuration of the SVPWM module. A three-phase 2-level inverter with dc link configuration can have eight possible switching states, which generates output voltage of the inverter. Each inverter switching state generates a voltage Space Vector (V_1 to V_6 active vectors, V_7 and V_8 zero voltage vectors) in the Space Vector plane (Figure: space vector diagram). The magnitude of each active vector (V_1 to V_6) is 2/3 V_{dc} (dc bus voltage). The Space Vector PWM (SVPWM) module inputs modulation index commands (U-Alpha and U-Beta) which are orthogonal signals (Alpha and Beta) as shown in Figure. The gain characteristic of the SVPWM module is given in Figure . The vertical axis of Figure represents the normalized peak motor phase voltage (V/V_{dc}) and the horizontal axis represents the normalized modulation index (M).

The inverter fundamental line-to-line RMS output voltage (V_{line}) can be approximated (linear range) by the following equation:

$$V_{line} = U_{mag} * MOD\_S_{Cl} * V_{dc} / \sqrt{6}/2^{25} \quad \ldots\ldots\ldots\ldots \quad (1)$$

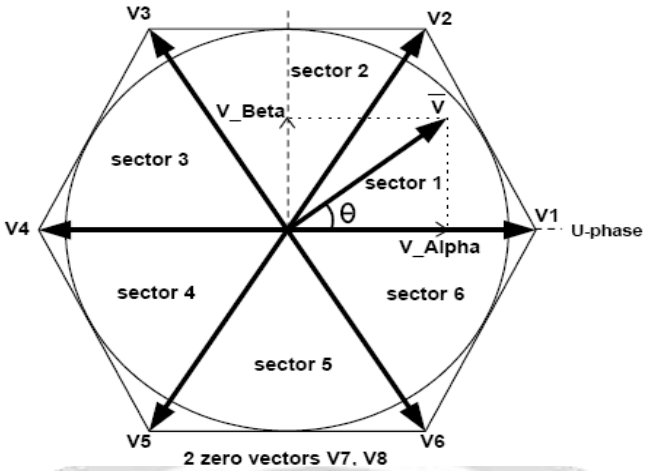

Fig-3: Space Vector Diagram.

This document is the property of International Rectifier and may not be copied or distributed without expressed consent. The maximum achievable modulation (U_{mag}_L) in the linear operating range is given by:

$$U_{mag}\text{-L} = 2^{25} * \sqrt{3}/\text{Mod\_S}_{Cl} \ldots\ldots\ldots\ldots \quad (2)$$

Over modulation occurs when modulation $U_{mag} > U_{mag}$_L. This corresponds to the condition where the voltage vector in (Figure: voltage vector rescaling) increases beyond the hexagon boundary. Under such circumstance, the Space Vector PWM algorithm will rescale the magnitude of the voltage vector to fit within the Hexagon limit. The magnitude of the voltage vector is restricted within the Hexagon; however, the phase angle (θ) is always preserved. The transfer gain (Figure: transfer characteristics) of the PWM modulator reduces and becomes non-linear in the over modulation region.

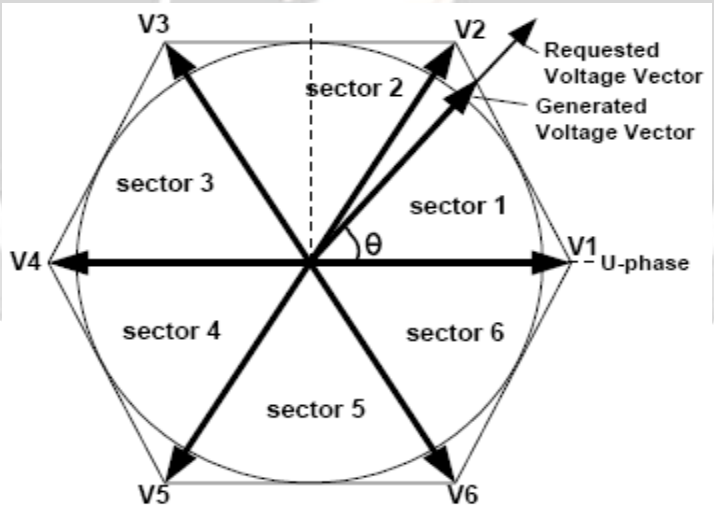

Fig-4: Voltage Vector Rescaling.

2.1 PWM Operation

Upon receiving the modulation index commands (U-Alpha and U-Beta) the sub-module SVPW M Tm starts its calculations at the rising edge of the PWM Load signal. The SVPWM _Tm module implements an algorithm that selects (based on sector determination) the active space vectors (V_1 to V_6) being used and calculates the appropriate time duration (with respect to one PWM cycle) for each active vector. The appropriated zero vectors are also being selected. The SVPWM_Tm module consumes 11 clock cycles typically and 35 clock cycles (worst case Tr) in over

modulation cases. At the falling edge of nSYNC, a new set of Space Vector times and vectors are readily available for actual PWM generation (Phase U, Phase V, Phase W) by sub module PWM Generation. It is crucial to trigger PWM Load at least 35 clock cycles prior to the falling edge of n SYNC signal; otherwise new modulation commands will not be implemented at the earliest PWM cycle.

The above Figures voltage vector rescaling illustrates the PWM waveforms for a voltage vector locates in sector I of the Space Vector plane (shown in Figure). The gating pattern outputs (PWMUH … PWMWL) include dead time insertion

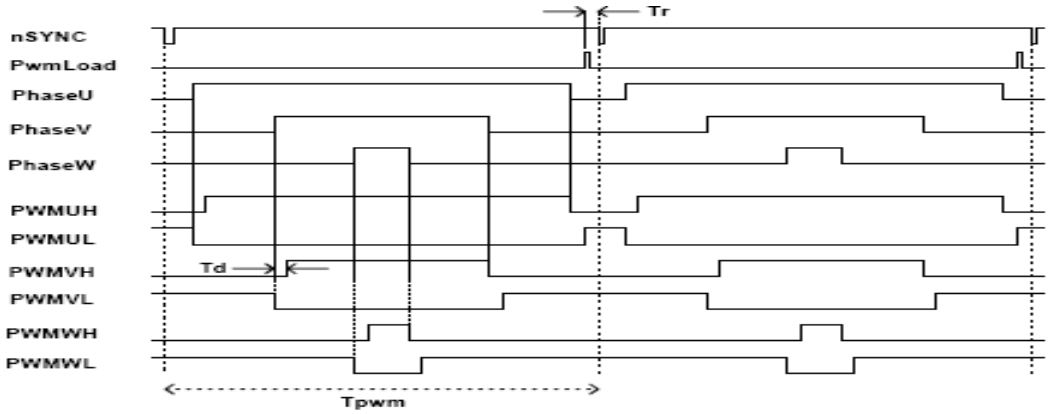

Fig-5: phase Space Vector PWM

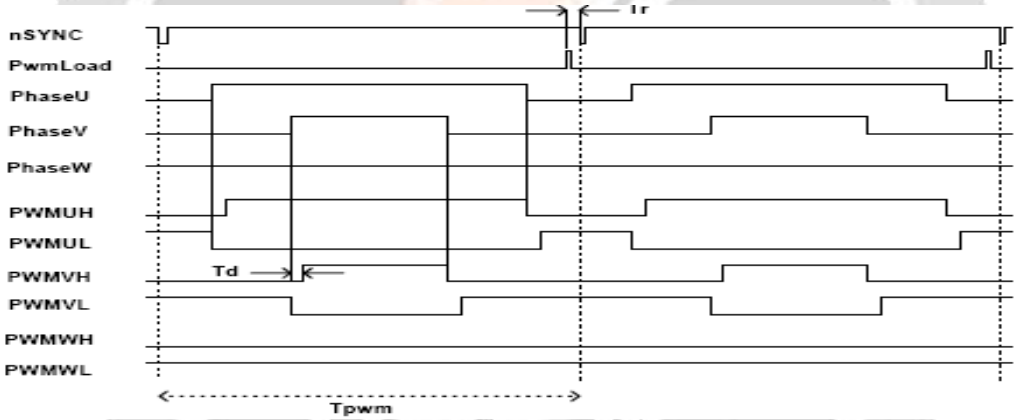

Fig-6: phase (6-step PWM) Space Vector PWM

3. PRINCIPLE OF OPERATION

Based on the discussions in Sections I and II, two new configurations of a three-level inverter to integrate battery storage and solar PV shown in Fig.5.1 are proposed, where no extra converter is required to connect the battery storage to the grid connected PV system. These can reduce the cost and improve the overall efficiency of the whole system particularly for medium and high power applications.

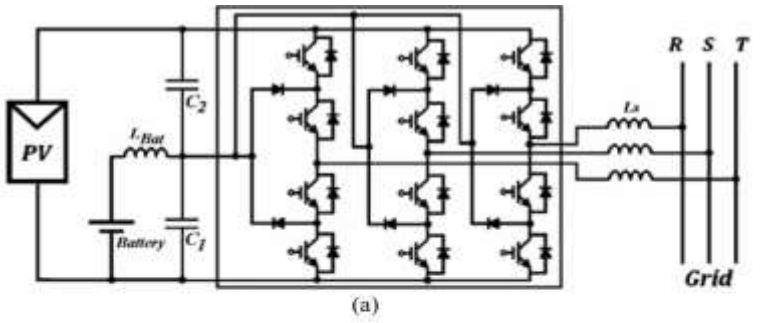

(a)

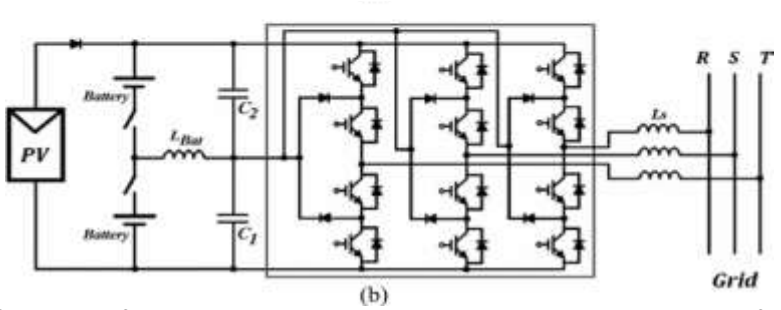

Fig-7: Proposed configurations for integrating solar PV and battery storage: (a) basic configuration; (b) improved configuration.

Fig. 5.1(a) shows the diagram of the basic configuration. In the proposed system, power can be transferred to the grid from the renewable energy source while allowing charging and discharging of the battery storage system as requested by the control system. The proposed system will be able to control the sum of the capacitor voltages (V_{c1} + V_{c2} = V_{dc}) to achieve the MPPT condition and at the same time will be able to control independently the lower capacitor voltage (V_{c1}) that can be used to control the charging and discharging of the battery storage system.
Further, the output of the inverter can still have the correct voltage waveform with low total harmonic distortion (THD) current in the ac side even under unbalanced capacitor voltages in the dc side of the inverter.
Although this configuration can operate under most conditions, however when the solar PV does not produce any power, the system cannot work properly with just one battery. Fig.5.1(b) shows the improved configuration where two batteries are now connected across two capacitors through two relays.
When one of the relays is closed and the other relay is open, the configuration in Fig.5.1(b) is similar to that in Fig.5.1(a) which can charge or discharge the battery storage while the renewable energy source can generate power. However, when the renewable energy is unavailable, both relays can be closed allowing the dc bus to transfer or absorb active and reactive power to or from the grid. It should be noted that these relays are selected to be ON or OFF as required; there is no PWM control requirement. This also provides flexibility in managing which of the two battery is to be charged when power is available from the renewable energy source or from the grid. When one of the batteries is fully charged, the relay connected to this battery can be opened while closing the relay on the other battery to charge. Special consideration needs to be made to ensure that current through the inductor *L* battery must be zero prior to opening any of these relays to avoid disrupting the inductor current and also to avoid damaging the relay.

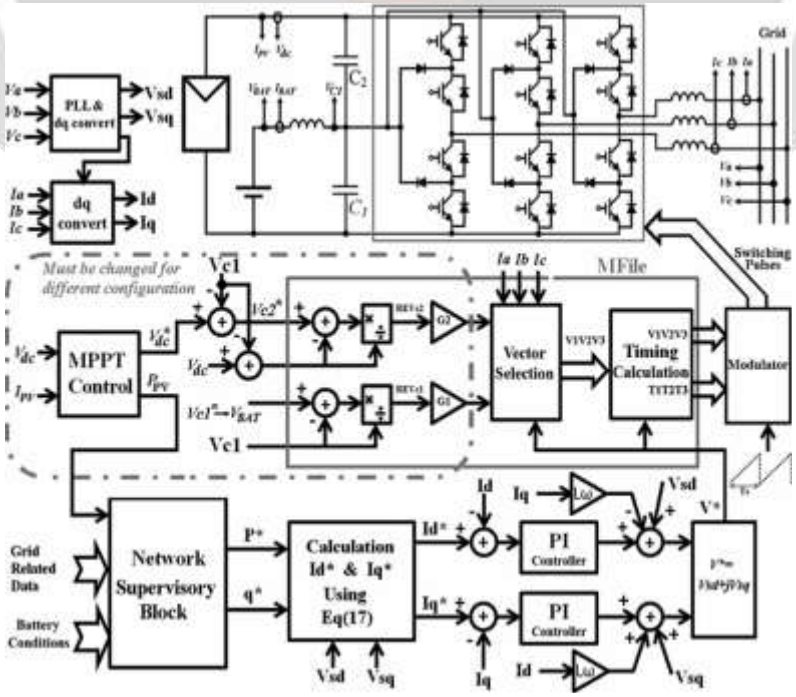

Fig-8: Control system diagram to integrate PV and battery storage.

3.1 Control Topology

In Fig.5.2(b), three different relay configurations can be obtained: 1) When the top relay is closed; 2) when the bottom relay is closed; and 3) when both relays are closed. Fig.5.2 shows the block diagram of the control system for configuration 1). In Fig.5.2, the requested active and reactive power generation by the inverter to be transferred to the grid will be determined by the network supervisory block. This will be achieved based on the available PV generation, the grid data, and the current battery variables. The MPPT block determines the requested dc voltage across the PV to achieve the MPPT condition. This voltage can be determined by using another control loop, with slower dynamics, using the measurement of the available PV power. The details of the MPPT algorithm to determine the desired voltage (V_{dc}). Based on the requested active (p) and reactive power (q), and the grid voltage in the d_q-axis, V_{sd} and V_{sq}, the requested inverter current in the d_q-axis, i_d and i_q can be obtained using

(17): $$P = V_{sd}\, i_d + V_{sq}\, i_q \; ; Q = V_{sq}\, i_d + V_{sd}\, i_q \quad \text{.....(17)}$$

where

$$i_d^* = p^* V_{sd} - q^* V_{sq} / V^*_{sd} + V^*_{sq}$$

$$i_q^* = q^* V_{sd} - p^* V_{sq} / V^*_{sq} + V^*_{sd}$$

By using a proportional and integral (PI) controller and decoupling control structure, the inverter requested voltage vector can be calculated. The proposed control system is shown in Fig.7. In the proposed system, to transfer a specified amount of power to the grid, the battery will be charged using surplus energy from the PV or will be discharged to support the PV when the available energy cannot support the requested power. After evaluating the requested reference voltage vector, the appropriate sector in the vector diagram can be determined. To determine which short vectors are to be selected, the relative errors of capacitor voltages given in (18) and (19) are used

$$eV_{c1} = V^*_{c1} - V_{c1}/V_{c1} \quad \text{.....(18)}$$

$$eV_{c2} = V^*_{c2} - V_{c2}/V_{c2} \quad \text{.....(19)}$$

Where V_{C1} and V_{C2} are the desired capacitor voltages, and $V_{C1}$and V_{C2} are the actual capacitor voltages for capacitor C_1 andC_2, respectively.

The selection of the short vectors will determine which capacitor is to be charged or discharged. To determine which short vector must be selected, the relative errors of capacitor voltages and their effectiveness on the control system behaviour are important. A decision function "F," as given in (20), can be defined based on this idea

$$F = G_1 e_{VC1} - G_2 e_{VC2} \qquad (20)$$

Where G_1 and G_2 are the gains associated with each of the relative errors of the capacitor voltages.G_1 and G_2 are used to determine which relative error of the capacitor voltages is more important and consequently allows better control of the chosen capacitor voltage. For example, for an application that requires the balancing of the capacitor voltages as in traditional three-level inverters, G_1 and G_2 must have the same value with equal reference voltage values, but in the proposed application where the capacitor voltages can be unbalanced, G_1 and G_2 are different and their values are completely dependent on their definitions of desired capacitor voltages. By using $V_{C2} = V_{dc} - V_{C1}$ and $V_{C1} = V_{BAT}$ and selecting G_2 much higher than G_1 , the PV can be controlled to the MPPT, and C_1 voltage can be controlled to allow charging and discharging of the battery. In each time step, the sign of F is used to determine which short vectors are to be chosen. When F is positive, the short vectors need to be selected that can charge C_1 or discharge C_2 in that particular time step by applying (14) and using similar reasoning to (15) and (16). Similarly, when F is negative, the short vectors need to be selected that can charge C_2 or discharge C_1 in that particular time step.

Based on the control system diagram given in Fig.5.2, on the ac side, the requested active power p, and reactive power q, will be generated by the inverter by implementing the requested voltage vector and applying the proper timing of the applied vectors. Further, on the dc side, MPPT control can be achieved by strict control of V_{c2} (G_2 - G_1) with reference value of ($V_{dc} - V_{c1}$) and more flexible control of V_{c1} with reference value of the battery voltage, V_{BAT}. By using the decision function (F) with the given reference values, the proper short vectors to be applied to implement the requested vector can be determined. With MPPT control, the PV arrays can transfer the maximum available power (P_{PV}), and with generating the requested vector in the ac side, the requested power P is transferred to the grid. Then, the control system will automatically control V_{C1} to transfer excess power ($P_{PV} - P$) to the battery storage or absorb the power deficit ($P - P_{PV}$) from the battery storage.

The same control system is applicable for configuration 2) by changing the generated reference voltages for the capacitors. Configuration 3) represents two storage systems connected to grid without any PV contribution, such as at night when the PV is not producing any output power.

4 SIMULATION RESULTS

A prototype system, is built in the lab to validate the operation and the effectiveness of the proposed system. The inverter and the control part of the prototype system is configurable to be used as a three-phase five-level floating capacitor based active neutral point clamp (5L-ANPC) inverter, a three-phase three-level ANPC inverter and a three-phase three-level NPC inverter applications. For the purpose of this paper, the prototype system is configured as a three-phase three-level NPC inverter. In this case, some of the switches will be continually set to OFF or ON. The output from the California Instruments programmable arbitrary waveform generator is used to emulate the grid and the output from a programmable solar array simulator (Elgar Terra SAS) from AMETEK is used to emulate the PV arrays. The Texas instrument TMS320F28335 control card and the Altera Cyclone IV EP4CE22F17C6 N FPGA card are used in the control board to provide the necessary control implementation ability. The implemented system specification is approximately similar to the same system configuration and values presented in the simulation section with the parameters given in Table I

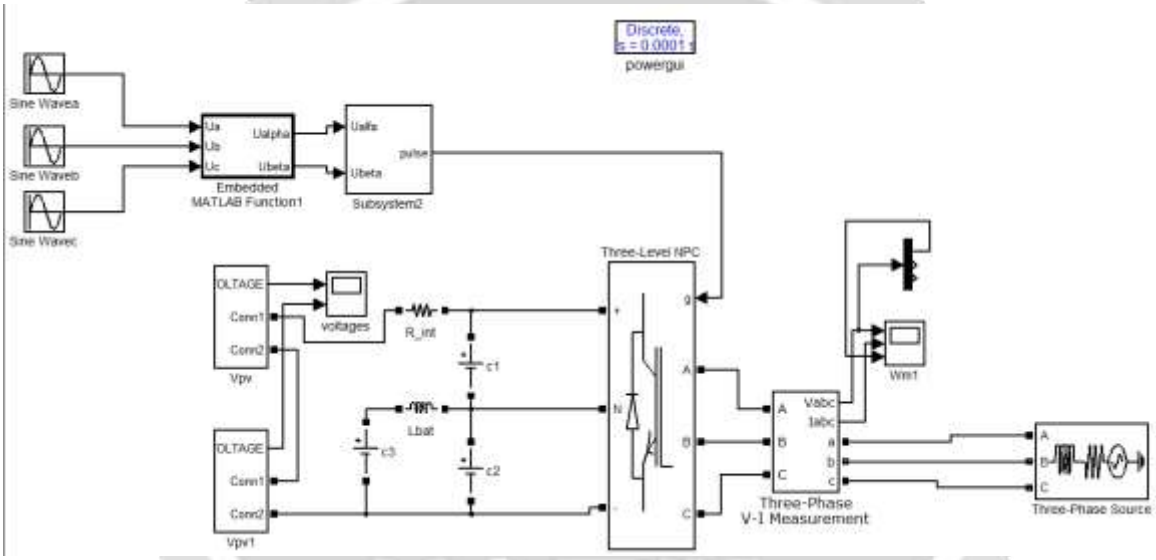

Fig-9: simulation of proposed system

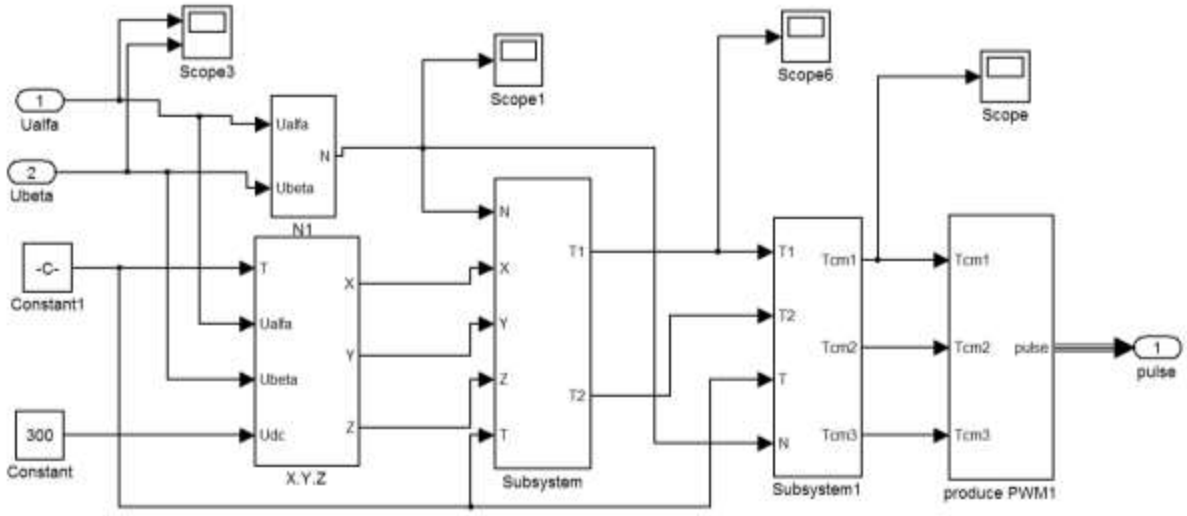

Fig-10: control circuit of proposed system.

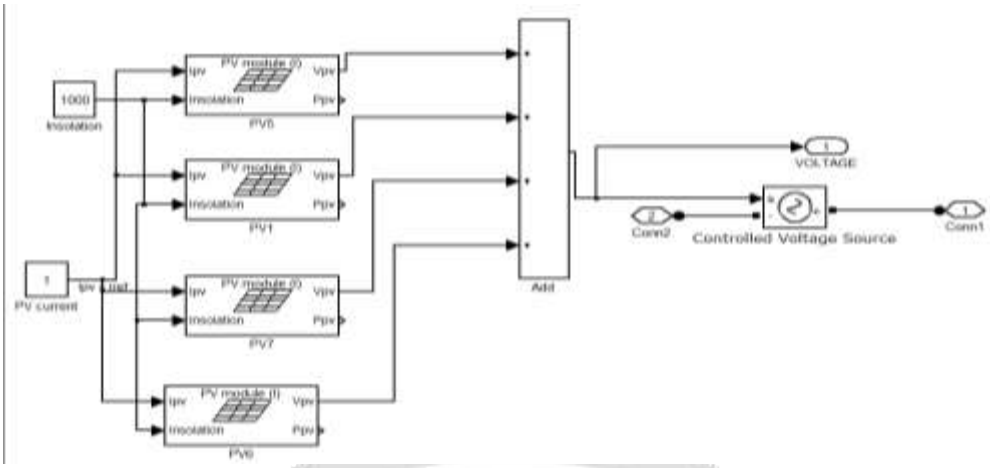

Fig-11: Solar PV design used in the system.

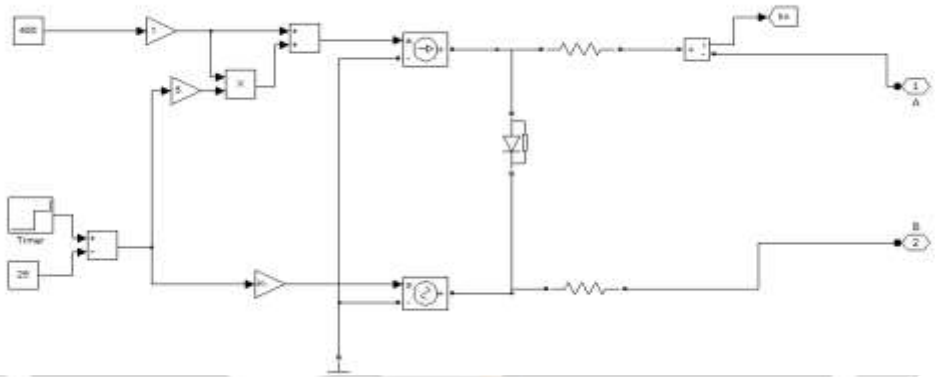

Fig-12: Equivalent circuit of the Battery model

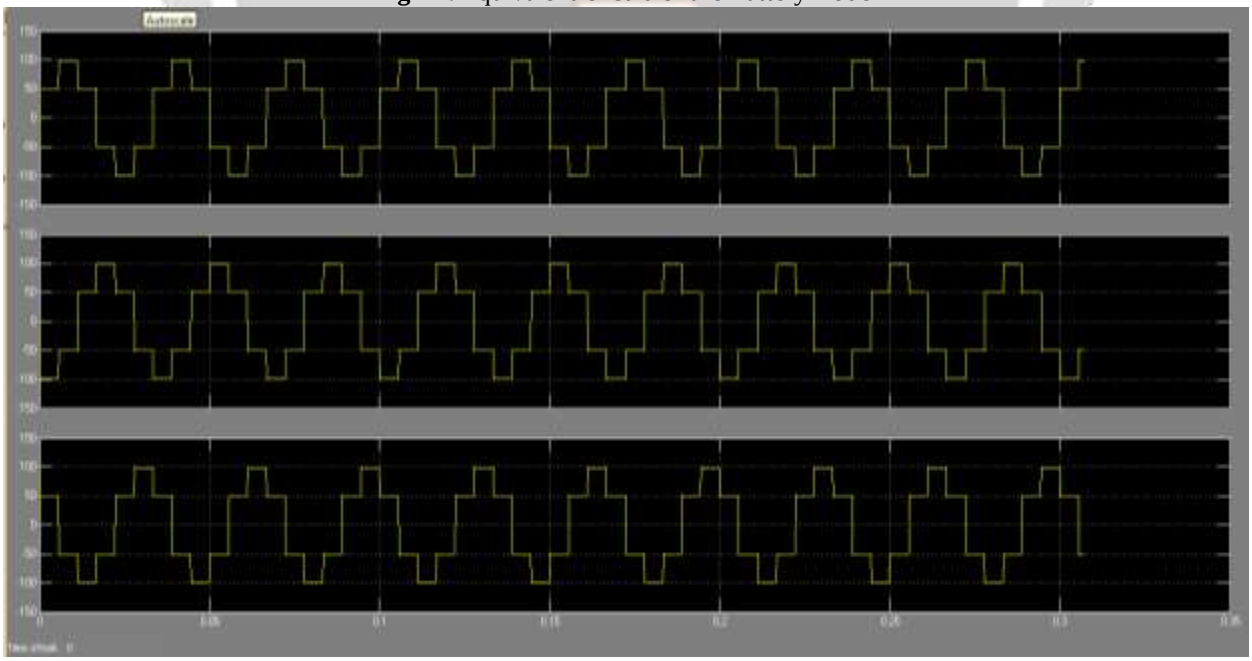

Fig-13: Phase Voltage waveform

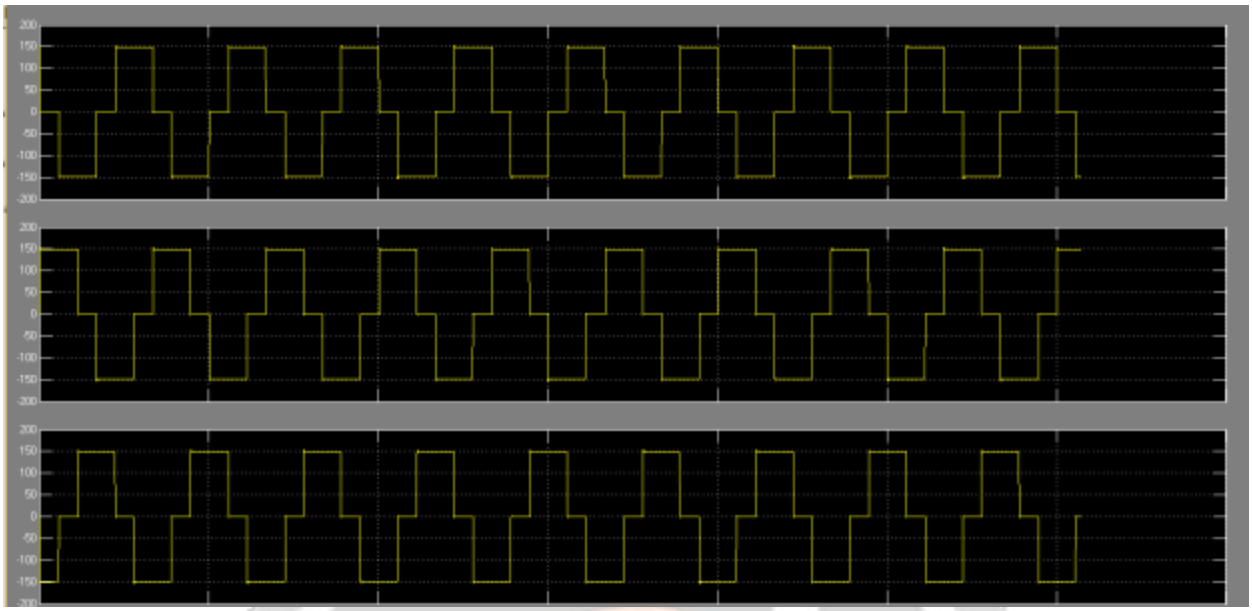

Fig-14: Line Voltage waveform

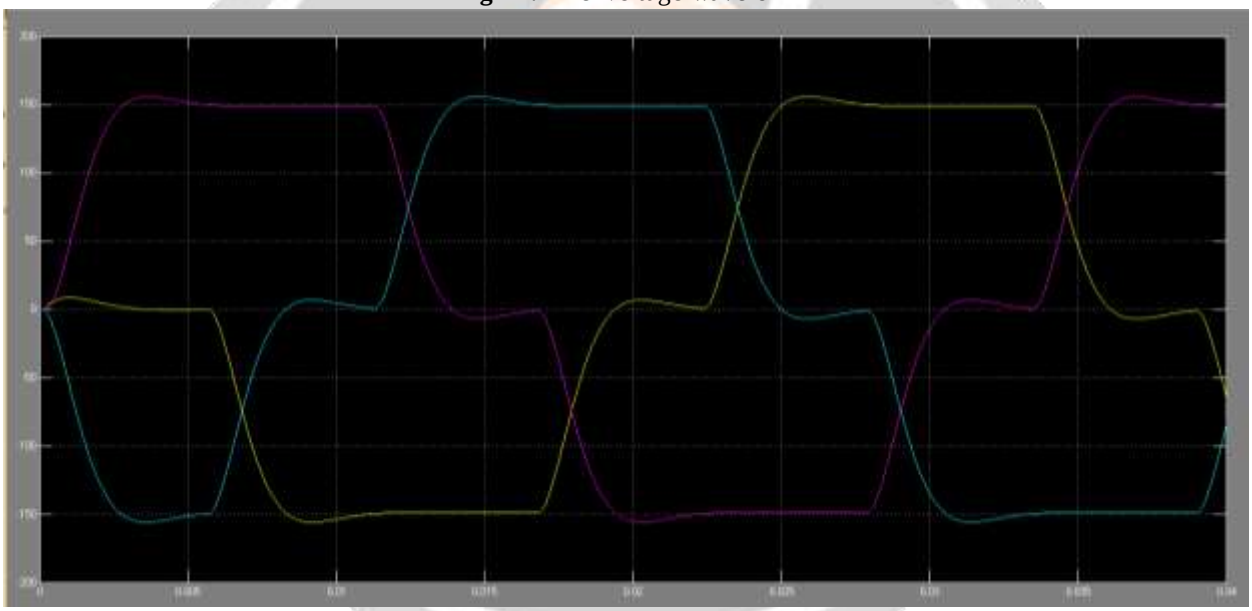

Fig-15: line current waveform

5. CONCLUSIONS

A simplified topology for a three-level NPC voltage source inverter that can integrate both renewable energy and battery storage on the dc side of the inverter has been presented. A theoretical framework of a novel extended unbalance three-level vector modulation technique that can generate the correct ac voltage under unbalanced dc voltage conditions has been proposed. Anew control algorithm for the proposed system has also been presented in order to control power flow between solar PV, battery, and grid system, while MPPT operation for the solar PV is achieved simultaneously. The effectiveness of the proposed topology and control algorithm was tested using simulations and results are presented. The results demonstrate that the proposed system is able to control ac-side current, and battery charging and discharging currents at different levels of solar irradiation. The results from experiments using a prototype built in the lab shave validated the proposed topology to control both PV and battery storage in supplying power to the ac grid.

6. REFERENCES

[1] O. Garc´ıa, J. A. Cobos, R. Prieto, P. Alou, and J. Uceda, "Single phase power factor correction: A survey," *IEEE Trans. Power Electron.*, vol. 18, no. 3, pp. 749–755, May 2003.
[2] M.M. Jovanovic andY. Jang, "State-of-the-art, single-phase, active power factor-correction techniques for high-power applications—An overview," *IEEE Trans. Ind. Electron.*, vol. 52, no. 3, pp. 701–708, Jun. 2005.
[3] D. S. L. Simonetti, J. Sebastian, and J. Uceda, "The discontinuous conduction mode SEPIC and CUK power factor pre regulators: Analysis and design," *IEEE Trans. Ind. Electron.*, vol. 44, no. 5, pp. 630–637, Oct.1997.
[4] M. Mahdavi and H. Farzanehfard, "Bridgeless SEPIC PFC rectifier with reduced components and conduction losses," *IEEE Trans. Ind. Electron.*, vol. 58, no. 9, pp. 4153–4160, Sep. 2011.
[5] A. A. Fardoun, E. H. Ismail, A. J. Sabzali, and M. A. Al-Saffar, "New efficient bridgeless Cuk rectifiers for PFC applications," *IEEE Trans. Power Electron.*, vol. 27, no. 7, pp. 3292–3301, Jul. 2012.
[6] E. H. Ismail, "Bridgeless SEPIC rectifier with unity power factor and reduced conduction losses," *IEEE Trans. Ind. Electron.*, vol. 56, no. 4, pp. 1147–1157, Apr. 2009.
[7] B. Su, J. Zhang, and Z. Lu, "Totem-pole boost bridgeless pfc rectifier with simple zero-current detection and full-range zvs operating at the boundary of DCM/CCM," *IEEE Trans. Power Electron.*, vol. 26, no. 2, pp. 427–435, Feb. 2011.
[8] J. Zhang, B. Su, and Z. Lu, "Single inductor three-level bridgeless boost power factor correction rectifier with nature voltage clamp," *IET Power Electron.*, vol. 5, no. 3, pp. 358–365, Mar. 2012.
[9] Y. Cho and J.-S. Lai, "Digital plug-in repetitive controller for single-phase bridgeless pfc converters," *IEEE Trans. Power Electron.*, vol. 28, no. 1, pp. 165–175, Jan. 2013.
[10] A. A. Fardoun, E. H. Ismail, A. J. Sabzali, and M. A. Al-Saffar, "Bridgeless resonant pseudo boost PFC rectifier," *IEEE Trans. Power Electron.*, vol. 29, no. 11, pp. 5949–5960, Nov. 2014.
[11] R. Gules, W. M. Santos, F. A. Reis, E. F. R. Romaneli, and A. A. Badin, "A modified SEPIC converter with high static gain for renewable applications," *IEEE Trans. Power Electron.*, vol. 29, no. 11, pp. 5860–5871, Nov. 2014.
[12] P. F. de Melo, R. Gules, E. F. R. Romaneli, and R. C. Annunziato, "A modified SEPIC converter for high-power-factor rectifier and universal input voltage applications," *IEEE Trans. Power Electron.*, vol. 25, no. 2, pp. 310–321, Feb. 2010.